



**HAL**  
open science

# Evolution of Indoor Cooking Emissions Captured by Using Secondary Electrospray Ionization High-Resolution Mass Spectrometry

Jiafa Zeng, Zhujun Yu, Majda Mekic, Jiangping Liu, Sheng Li, Gwendal Loisel, Wei Gao, Adrien Gandolfo, Zhen Zhou, Xinming Wang, et al.

► **To cite this version:**

Jiafa Zeng, Zhujun Yu, Majda Mekic, Jiangping Liu, Sheng Li, et al.. Evolution of Indoor Cooking Emissions Captured by Using Secondary Electrospray Ionization High-Resolution Mass Spectrometry. Environmental Science and Technology Letters, 2020, 7 (2), pp.76-81. 10.1021/acs.estlett.0c00044 . hal-03151910

**HAL Id: hal-03151910**

**<https://hal.science/hal-03151910>**

Submitted on 25 Feb 2021

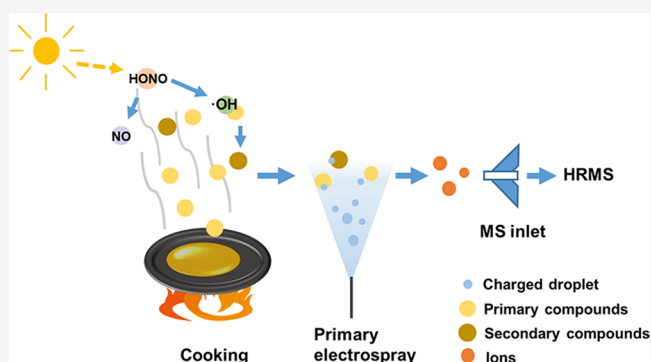
**HAL** is a multi-disciplinary open access archive for the deposit and dissemination of scientific research documents, whether they are published or not. The documents may come from teaching and research institutions in France or abroad, or from public or private research centers.

L'archive ouverte pluridisciplinaire **HAL**, est destinée au dépôt et à la diffusion de documents scientifiques de niveau recherche, publiés ou non, émanant des établissements d'enseignement et de recherche français ou étrangers, des laboratoires publics ou privés.

# Evolution of Indoor Cooking Emissions Captured by Using Secondary Electrospray Ionization High-Resolution Mass Spectrometry

Jiafa Zeng, Zhujun Yu, Majda Mekic, Jiangping Liu, Sheng Li, Gwendal Loisel, Wei Gao, Adrien Gandolfo, Zhen Zhou, Xinming Wang, Hartmut Herrmann, Sasho Gligorovski,\* and Xue Li\*

**ABSTRACT:** Cooking emissions represent a major source of air pollution in the indoor environment and exhibit adverse health effects caused by particulate matter together with volatile organic compounds (VOCs). A multitude of unknown compounds are released during cooking, some of which play important roles as precursors of more hazardous secondary organic aerosols in indoor air. Here, we applied secondary electrospray ionization high-resolution mass spectrometry for real-time measurements of VOCs and particles from cooking peanut oil in the presence of 300 ppbv nitrogen oxides ( $\text{NO}_x$ ) generated by a gas stove in an indoor environment. More than 600 compounds have been found during and after cooking, including N-heterocyclic compounds, O-heterocyclic compounds, aldehydes, fatty acids, and oxidation products. Approximately 200 compounds appeared after cooking and were hence secondarily formed products. The most abundant compound was 9-oxononanoic acid ( $\text{C}_9\text{H}_{16}\text{O}_3$ ), which is likely the product formed during the heterogeneous hydroxyl (OH) radical oxidation of oleic acid ( $\text{C}_{18}\text{H}_{34}\text{O}_2$ ) or linoleic acid ( $\text{C}_{18}\text{H}_{32}\text{O}_2$ ). Real-time detection of an important number of organic compounds in indoor air poses a challenge to indoor air quality and models, which do not account for this extremely large range of compounds.



## 1. INTRODUCTION

Combustion processes such as gas stove cooking represent some of the most important temporal sources of air pollution in the indoor environment. A large number of organic particles and volatile organic compounds (VOCs) are released,<sup>1</sup> many of which exhibit adverse health effects.<sup>2–5</sup> Cooking fumes contain a wide range of compounds, such as alkanes, alkenes, aldehydes, and fatty acids.<sup>6–10</sup> Cooking also releases large amounts of nitrogen oxides ( $\text{NO}_x$ ) and nitrous acid (HONO) into the indoor air.<sup>11–14</sup> Recently, it has been demonstrated that HONO can be easily photodissociated in indoor air by the ultraviolet (UV) fraction of sunlight filtered through the windows<sup>15,16</sup> and generate hydroxyl (OH) radicals at the level of  $\sim 10^6 \text{ cm}^{-3}$ .<sup>14,17</sup> The compounds in cooking fumes can react with highly reactive OH radicals, forming secondary organic compounds. This is assumed to be similar to the formation of secondary products by reactions of OH radicals with VOCs and organic particles in the outdoor atmosphere, which is known and has been experimentally verified.<sup>18–21</sup> Some of these secondary products have lower volatility and are more toxic than the initially emitted VOCs.<sup>22</sup> Real-time measurements of compounds formed upon reaction of OH radicals with primary emissions from cooking have been attracting more attention in recent years,<sup>23,24</sup> but only a few studies have

been reported to date.<sup>25</sup> This can be partially explained by the complexity of these reaction processes and also by the limitations in the analytical tools.

Secondary electrospray ionization high-resolution mass spectrometry (SESI-HRMS) is a novel ambient MS technique and shows great potential in capturing the evolution of compounds in real time.<sup>26</sup> The application of SESI especially favors the detection of reactive compounds, such as fatty acids, aldehydes, ketones, etc.;<sup>27</sup> furthermore, accurate identification of compounds can be realized by HRMS. Recently, via application of SESI-HRMS to real-time breath analysis, around 1000 breath compounds per subject have been measured and unambiguously identified.<sup>28</sup>

In this study, SESI-HRMS was applied for the first time to measure the primary emissions from cooking fumes and the real-time evolutions of primary and secondary organic compounds in an indoor environment. The literature suggests that high levels of OH radicals can be produced upon

photodissociation of HONO, which determine the oxidation capacity of indoor air.<sup>14</sup> Thus, the ultimate goal of this study is to identify the secondarily formed products upon reaction of OH radicals with the primarily emitted organic compounds in the gas phase and particulate phase in the indoor air.

## 2. MATERIALS AND METHODS

**2.1. Experimental Setup.** Measurements were conducted in a 23 m<sup>3</sup> room with a window (0.99 m<sup>2</sup>) facing southeast at our institute (Figure S1). The sunlight irradiated the room through the window during certain periods of the day. Peanut oil was heated in a pan on a natural gas stove (ZB-16M, Iwatani) for ~10 min, and then the gas stove was turned off. Two fans were placed at two corners of the room (Figure S1) to ensure the indoor air was homogeneously mixed during the experiments. An air exchange rate of ~0.6 h<sup>-1</sup> was estimated from the evolution of the carbon dioxide (CO<sub>2</sub>) from combustion (details in the Supporting Information) applying the procedure described elsewhere.<sup>14</sup> The photostationary state (PSS) approach<sup>17,29</sup> was used to estimate the time profiles of OH radical values. Details about the estimations of OH radical values can refer to our previous work<sup>14</sup>, including the measurements of spectral irradiance, NO<sub>x</sub>, HONO, and ozone (O<sub>3</sub>). The measured O<sub>3</sub> values during the campaign were below 200 parts per trillion by volume (pptv), and therefore, ozonolysis of alkenes as an OH source can be neglected. A control experiment was performed under the same condition but without cooking; each set of measurements was repeated at least twice.

**2.2. SESI-HRMS Analysis of Emissions.** A homemade SESI source was coupled to a high-resolution quadrupole Orbitrap mass spectrometer (Thermo Scientific).<sup>30</sup> Cooking emissions were delivered through a 6.7 m long Teflon tube (4 mm inside diameter) at a rate of 1.4 L min<sup>-1</sup>. Samples without pretreatment were introduced into the SESI-HRMS instrument in real time for direct ionization (Figure S1).<sup>29</sup> Compounds were detected at a time resolution of 1 s in fast polarity-switching mode, and ESI voltages were set to 2.5 and -2.5 kV. The scan range is *m/z* 50–500, and the mass resolution is 140000 at *m/z* 255. The limit of detection (LOD) and sensitivity of SESI-HRMS, sampling efficiency, and delay of the 6.7 m sampling line were evaluated by using a set of gas standards (details in Text S1 and Table S1). The LODs range from pptv to parts per billion by volume (ppbv), which agree with the previous studies.<sup>31</sup> The sampling efficiencies are 4–28% and 14–49% for 2 and 20 ppbv standard compounds, respectively. The sampling efficiencies vary greatly from compound to compound, and thus we compared the signal intensities only within individual compounds instead of between compounds. Because <200 pptv O<sub>3</sub> was detected in this indoor environment, O<sub>3</sub>-induced heterogeneous chemistry in the Teflon tubing can be neglected. Prior to measurements, the mass spectrometer was calibrated with the commercial standard calibration solutions (Thermo Scientific; details in Text S1).

**2.3. Data Analysis.** The raw data from SESI-HRMS were pretreated with a Python program named BreathFinder to obtain a data matrix, including *m/z* values, signal intensities, and time points of all of the ions detected (details in the Supporting Information). Then, the data matrix was further investigated by using cluster analysis in Matlab R2018b and Kendrick Mass Defect (KMD) analysis.<sup>32</sup> KMD analysis is especially suitable for the data acquired by HRMS to show

visualized trends in the elemental compositions of complex organic compounds.<sup>33</sup> The Kendrick mass (KM) and KMD are calculated as follows:

$$\text{KM} = \text{IUPAC mass} \times (14/14.01565) \quad (1)$$

$$\text{KMD} = \text{nominal KM} - \text{exact KM} \quad (2)$$

where 14.01565 is the exact mass of the CH<sub>2</sub> unit and 14 is the nominal mass.

Thus, compounds that have the same general molecular formula (e.g., C<sub>*n*</sub>H<sub>2*n*</sub>O<sub>2</sub>) but differ in the number of the base units (such as CH<sub>2</sub> groups) have identical KMD values and thus lie on the same horizontal line in the plot of KM versus KMD. The elemental composition of each compound used in KMD analysis was obtained using Xcalibur (version 4.2.28.14, Thermo).

The enhancement ratio (ER) was used to evaluate the enhancement of the signal intensity of a compound during cooking; ER is calculated on the basis of the maximum signal intensity of a compound and its signal intensity at the beginning of the cooking experiment.

## 3. RESULTS AND DISCUSSION

**3.1. Evolution of Cooking Emissions.** By using SESI-HRMS, an important number of reported compounds have been detected, such as aldehydes, fatty acids, N-heterocyclic compounds, and O-heterocyclic compounds (Figure S2). Obvious differences were found between mass spectral fingerprints before, during, and after cooking (Figure S3). To determine how many groups of compounds were emitted from cooking, 864 ions with intensities of  $\geq 1 \times 10^5$  au captured in real time were further investigated using cluster analysis. Six groups (657 ions in total) characterized with different chronological variations are presented in Figure 1, which have not been observed in the control experiment (Figure S5). In addition, to explore the evolution of primary emissions and the formation of secondarily formed products, molecular formulas were assigned to the ions detected (Tables S2–S7),

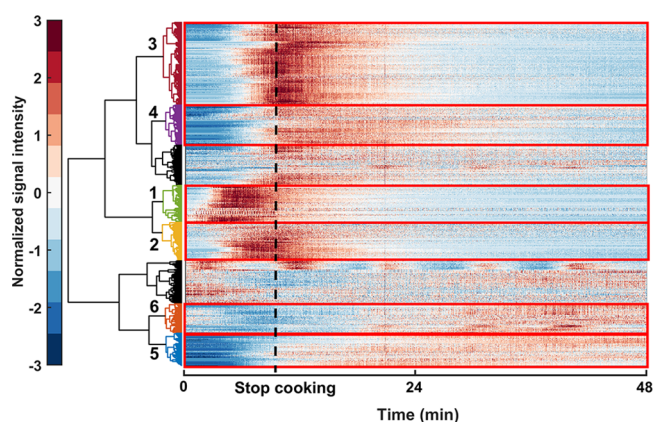


**Figure 1.** Cluster analysis of 864 ions with signal intensities of  $\geq 1 \times 10^5$  au during and after cooking. Six groups distinguished by cluster analysis are numbered according to the order at which they reached their peak levels and represented by different colors: group 1, green; group 2, yellow; group 3, wine red; group 4, purple; group 5, blue; group 6, orange; background, black. The normalized signal intensity is presented by a color-coded scale; i.e., the signal intensity increases from dark blue (normalized value of -3) to wine red (normalized value of 3).

and ER values were provided for some of these compounds (Table S8). For example, compounds in group 1 (93 ions) are characterized by reaching the peak level during cooking. Most of the N-heterocyclic compounds, e.g., trimethylpyrazine (ER = 3.0) and 3-methoxy-4-pyridine (ER = 3.2), were identified in this group, which are consistent with the flavor components with low boiling points in peanut oil during cooking.<sup>34,35</sup> Compounds in groups 2 (97 ions) and 3 (208 ions) achieved the maximum signal intensity around the time when the gas stove was turned off. These two groups mainly contain unsaturated aldehydes and O-heterocyclic compounds that are formed by chemical processes involved in the oil heating, inducing the breaking bonds of the fatty acids.<sup>4</sup> Polyunsaturated fatty acids such as linoleic acid (LA) can readily undergo autoxidation<sup>36</sup> and generate the unsaturated aldehyde decadienal in peanut oil.<sup>37</sup> 2,4-Decadienal (ER = 155.1), which exhibits the second highest signal intensity, is genotoxic to human lung cells and increases the carcinogenic risk of inhabitants.<sup>38–40</sup> O-Heterocyclic compounds like 2-acetyl-5-methylfuran (ER = 4.9) and 5-propyldihydro-2(3H)-furanone (ER = 5.4) are flavor compounds found during thermal processing of foods<sup>41</sup> and thus can be used as tracers for cooking emission.<sup>42</sup>

Most of the unsaturated and saturated fatty acids were classified into groups 4 (101 ions) and 5 (82 ions). Oleic acid (OA,  $C_{18}H_{34}O_2$ ) and palmitic acid ( $C_{16}H_{32}O_2$ ; ER = 106.8) are the most abundant unsaturated fatty acid and saturated fatty acid, respectively. It is noteworthy that OA was detected in the particle phase and its peak level is ~60% of the palmitic acid signal intensity. Furthermore, the signal intensities of unsaturated fatty acids decreased faster than those of saturated fatty acids after the gas stove had been turned off (Figure S4). This is reasonable because compared to saturated fatty acids, unsaturated fatty acids are more easily oxidized by OH radicals or  $O_3$  due to the reactions with the C=C bond. The addition of OH to the C=C bond is found to be the dominant reaction pathway for unsaturated compounds.<sup>43</sup> The uptake coefficients for the reactions of OH radicals with unsaturated compounds are also much larger than those of the OH reactions with saturated fatty acids.<sup>43</sup> Moreover, both unsaturated and saturated fatty acids contribute to the formation of SOA in the indoor environment as they are established precursors of SOA in the atmosphere.<sup>9,44</sup> The compounds in group 6 (76 ions) represent a mixture of oxidation products and “background” compounds emerging from typical indoor materials (furniture, walls, etc.) that were present in the air before the experiments started. For example, the peak at  $m/z$  60.0816 is assigned to trimethylamine (TMA,  $C_3H_9N$ ; ER = 54.7) and might be the product of choline in the peanut oil through thermal decomposition.<sup>45</sup> TMA can potentially form SOA during gas-phase reactions with OH radicals,  $O_3$ , and  $NO_3$ .<sup>46–48</sup> The peak at  $m/z$  133.1335 ( $C_6H_{16}ON_2$ ; ER = 95.3) shows a trend very similar to that of the TMA profile (Figure S6), which might be a product from TMA. The  $NO_x$  mixing ratio reached ~300 ppbv during cooking,<sup>14</sup> which is also comparable with the previous reports.<sup>11,12</sup> For the background compounds, the intensities decreased during cooking and then returned to the initial level after cooking.

**3.2. Formation of Secondary Compounds.** A total of 526 ions were detected as new products resulting from cooking, among which 229 ions were detected after cooking. By using KMD analysis, a series of homologous series were distinguished (Figure 2 and Figures S6–S8). Taking the ions

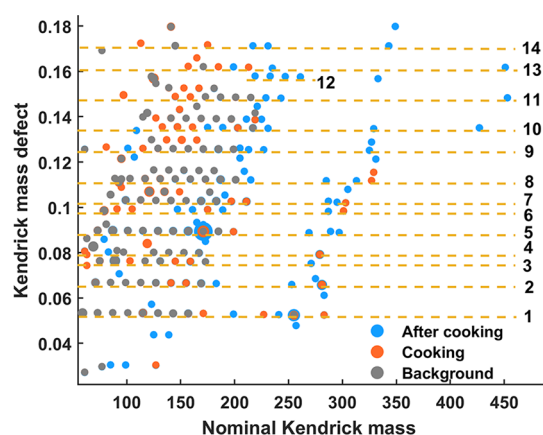


**Figure 2.**  $CH_2$  KMD vs nominal KM of odd  $m/z$  values of ions detected in the negative ion detection mode during cooking (orange dots) and after cooking (blue dots). Ions found in the background (gray dots) represent compounds observed in the control experiments. The compounds that have the same general molecular formula but different numbers of  $CH_2$  group appear on the same horizontal line: line 1,  $C_nH_{2n}O_2$ ; line 2,  $C_nH_{2n-2}O_2$ ; line 3,  $C_nH_{2n}O_3$ ; line 4,  $C_nH_{2n-4}O_2$ ; line 5,  $C_nH_{2n-2}O_3$ ; line 6,  $C_nH_{2n}O_4$ ; line 7,  $C_nH_{2n-8}O_2$ ; line 8,  $C_nH_{2n-2}O_4$ ; line 9,  $C_nH_{2n-4}O_4$ ; line 10,  $C_nH_{2n-2}O_5$ ; line 11,  $C_nH_{2n-4}O_5$ ; line 12,  $C_nH_{2n-2}O_6$ ; line 13,  $C_nH_{2n-6}O_5$ ; line 14,  $C_nH_{2n-4}O_6$ .

with odd  $m/z$  values for example, we identified 14 homologous series of compounds containing a carbon atom (C), a hydrogen atom (H), and an oxygen atom (O) (Figure 2). Most of these compounds were found as fatty acids and their oxidation products. For example, compounds on line 1 are saturated fatty acids ( $C_nH_{2n}O_2$ ), and those on line 2 are monounsaturated fatty acids ( $C_nH_{2n-2}O_2$ ).

Because the mechanism of heterogeneous OH oxidation of OA has been well studied,<sup>43,49,50</sup> all of the known intermediate and final products were carefully examined. On the basis of the accurate mass and isotopic pattern, LA, OA, and their intermediate and final products have been distinguished unambiguously, including  $C_{18}H_{34}O_2$  [ $m/z$  281.2483, OA, line 2 (Figure 2)],  $C_{18}H_{32}O_2$  [ $m/z$  279.2326, LA, line 4 (Figure 2)],  $C_{18}H_{35}O_5$  ( $m/z$  330.2408),  $C_{18}H_{35}O_4$  ( $m/z$  314.2459),  $C_{18}H_{34}O_3$  [ $m/z$  297.2429, line 5 (Figure 2)],  $C_9H_{16}O_4$  [ $m/z$  187.0967, azelaic acid, AA, line 8; ER = 45.5 (Figure 2)], and  $C_9H_{16}O_3$  [ $m/z$  171.1017, 9-oxononanoic acid, 9-ON, line 5; ER = 207.7 (Figure 2)]. Some compounds from line 10 (e.g.,  $C_{18}H_{34}O_5$ ,  $m/z$  329.2329) to line 14 (e.g.,  $C_{18}H_{32}O_6$ ,  $m/z$  343.2120) in Figure 2 are likely produced by addition of OH to the C=C bond of polyunsaturated fatty acids like LA.<sup>50</sup> Temporal evolution profiles of these compounds have also been captured in real time (Figure 3); among all of the secondary products, 9-ON shows the highest signal intensity. The temporal profiles of OA, LA, and OH radicals are similar to each other, and meanwhile, the signal intensities of 9-ON and AA increase continuously after cooking, implying that 9-ON and AA are formed via the heterogeneous reaction of OH with OA or LA. However, the possibility that AA and 9-ON can also be formed by the reaction of OA or LA with  $O_3$  in indoor air that exhibits higher ozone concentrations (in this study, the  $O_3$  mixing ratio was <200 pptv) cannot be excluded.<sup>51,52</sup> To illustrate the importance of OH radical reactions, we performed a simple calculation based on the reactivity of  $O_3$  and OH radical on the particle surface<sup>50,53</sup> to compare the lifetimes of OA by reactions with OH radical and

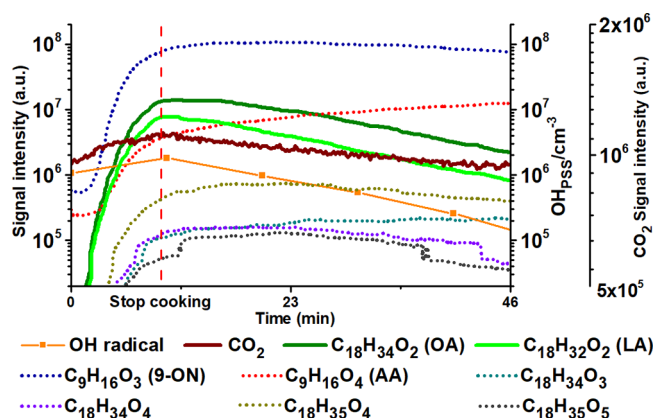


**Figure 3.** Time–intensity profiles of primarily emitted OA, LA, and products of OA or LA by OH oxidation, signal intensities of CO<sub>2</sub>, and estimated OH radical concentrations.<sup>14</sup>

O<sub>3</sub> and removal of OA by air exchange with outdoor air. The calculations show that the most important removal process for OA is the reaction with the OH radical, because the effective uptake coefficient was reported to be  $1.72 \pm 0.08$ , indicating particle-phase secondary chain chemistry.<sup>50</sup> Removal by reactions with O<sub>3</sub> would take  $\sim 13$  min ( $k_{\text{first}} = 1.31 \times 10^{-3} \text{ s}^{-1}$ ),<sup>51</sup> and removal by air exchange would take 1.6 h (taking the average exchange rate calculated in this work of  $1.7 \times 10^{-4} \text{ s}^{-1}$ ). The uptake coefficient of OH on LA is even higher than that on OA ( $3.75 \pm 0.18$ ), and the reaction of O<sub>3</sub> with LA ( $k_{\text{first}} = 4.4 \times 10^{-4} \text{ s}^{-1}$ ) is slower than that with OA, indicating that the removal of OA and LA is driven by OH radical chemistry. 9-ON and AA are most likely formed through the OH oxidation of OA, LA, or both simultaneously.

In conclusion, by using a novel real-time MS technique SESI-HRMS, a number of primary cooking emissions and secondary products formed upon reactions with OH radicals in indoor air have been detected and identified. High-temporal resolution data make it possible to monitor primary compounds and their intermediate and final products during and after cooking. In terms of OA, for example, 9-ON and AA, two well-known SOA materials,<sup>44,54,55</sup> were identified as secondary products of OA due to OH reaction. We have demonstrated that OH radical reactions occur indoors as predicted in previous studies.<sup>17,22</sup> We strongly recommend a future model study to better predict the formation of secondary products through reactions of O<sub>3</sub> and OH with primarily emitted organic compounds in indoor air; many secondary products formed through OH radical reactions can be even more toxic than the primarily emitted organic compounds.<sup>2</sup> This is especially important considering that a recent model study<sup>56</sup> predicted that although OH radicals produced by HONO photolysis are located only in the sunlit regions of the indoor environment, the oxidation products are relatively well distributed in the entire room.

## ■ ASSOCIATED CONTENT

### Supporting Information

The Supporting Information is available free of charge at <https://pubs.acs.org/doi/10.1021/acs.estlett.0c00044>.

Detailed information about the cooking experiments and data analysis (Text S1); detection limit and sensitivity of SESI-HRMS, and sampling efficiency of the 6.7-m sampling tube (Table S1); detailed information about

ions classified in six different groups (Tables S2–S7); detailed information about the enhancement ratio (ER) of identified compounds (Table S8); graphical illustration of the experimental room (Figure S1); temporal profiles of unsaturated aldehydes, unsaturated fatty acids, saturated fatty acids, and N-heterocyclic compounds from cooking (Figure S2); mass spectral fingerprints of the peanut oil heating experiment (Figure S3); time–signal intensity profiles of saturated and unsaturated fatty acids (Figure S4); cluster plot of ions detected during the control experiment (Figure S5); temporal profiles of ions detected at  $m/z$  60.0816 and 133.1335 (Figure S6); and KMD plots of even and odd  $m/z$  values of ions detected in negative and positive ion detection mode (Figures S7–S9) (PDF)

## ■ AUTHOR INFORMATION

### Corresponding Authors

**Sasho Gligorovski** – State Key Laboratory of Organic Geochemistry, Guangzhou Institute of Geochemistry, Chinese Academy of Sciences, Guangzhou 510640, China; [orcid.org/0000-0003-4151-2224](https://orcid.org/0000-0003-4151-2224); Phone: +86-20-85291497; Email: [gligorovski@gig.ac.cn](mailto:gligorovski@gig.ac.cn)

**Xue Li** – Institute of Mass Spectrometry and Atmospheric Environment, Guangdong Provincial Engineering Research Center for On-line Source Apportionment System of Air Pollution, Jinan University, Guangzhou 510632, China; [orcid.org/0000-0001-9247-0584](https://orcid.org/0000-0001-9247-0584); Phone: +86-20-85221076; Email: [tamylee@jnu.edu.cn](mailto:tamylee@jnu.edu.cn)

### Authors

**Jiafa Zeng** – Institute of Mass Spectrometry and Atmospheric Environment, Guangdong Provincial Engineering Research Center for On-line Source Apportionment System of Air Pollution, Jinan University, Guangzhou 510632, China; [orcid.org/0000-0002-9425-0371](https://orcid.org/0000-0002-9425-0371)

**Zhujun Yu** – Institute of Mass Spectrometry and Atmospheric Environment, Guangdong Provincial Engineering Research Center for On-line Source Apportionment System of Air Pollution, Jinan University, Guangzhou 510632, China

**Majda Mekic** – State Key Laboratory of Organic Geochemistry, Guangzhou Institute of Geochemistry, Chinese Academy of Sciences, Guangzhou 510640, China; University of Chinese Academy of Sciences, Beijing 10069, China

**Jiangping Liu** – State Key Laboratory of Organic Geochemistry, Guangzhou Institute of Geochemistry, Chinese Academy of Sciences, Guangzhou 510640, China; University of Chinese Academy of Sciences, Beijing 10069, China

**Sheng Li** – State Key Laboratory of Organic Geochemistry, Guangzhou Institute of Geochemistry, Chinese Academy of Sciences, Guangzhou 510640, China; University of Chinese Academy of Sciences, Beijing 10069, China

**Gwendal Loisel** – State Key Laboratory of Organic Geochemistry, Guangzhou Institute of Geochemistry, Chinese Academy of Sciences, Guangzhou 510640, China

**Wei Gao** – Institute of Mass Spectrometry and Atmospheric Environment, Guangdong Provincial Engineering Research Center for On-line Source Apportionment System of Air Pollution, Jinan University, Guangzhou 510632, China

**Adrien Gandolfo** – CNRS, LCE, UMR 7376, Aix Marseille Univ, 13331 Marseille, France

**Zhen Zhou** – Institute of Mass Spectrometry and Atmospheric Environment, Guangdong Provincial Engineering Research

Center for On-line Source Apportionment System of Air Pollution, Jinan University, Guangzhou 510632, China

**Xinming Wang** – State Key Laboratory of Organic Geochemistry, Guangzhou Institute of Geochemistry, Chinese Academy of Sciences, Guangzhou 510640, China; [orcid.org/0000-0002-1982-0928](https://orcid.org/0000-0002-1982-0928)

**Hartmut Herrmann** – School of Environmental Science and Engineering, Shandong University, Qingdao 266237, China; Shanghai Key Laboratory of Atmospheric Particle Pollution and Prevention, Department of Environmental Science & Engineering, Institute of Atmospheric Sciences, Fudan University, Shanghai 200433, China; Atmospheric Chemistry Department (ACD), Leibniz-Institute for Tropospheric Research (TROPOS), 04318 Leipzig, Germany; [orcid.org/0000-0001-7044-2101](https://orcid.org/0000-0001-7044-2101)

Complete contact information is available at:

<https://pubs.acs.org/10.1021/acs.estlett.0c00044>

### Author Contributions

J.Z., Z.Y., and M.M. contributed equally to this work.

### Notes

The authors declare no competing financial interest.

### ACKNOWLEDGMENTS

This study was funded by the Science and Technology Program of Guangzhou (201804010114), the National Natural Science Foundation of China (41773131 and 41977187), and Major Projects of the Ministry of Science and Technology of China (2016YFC0201002). The authors are very grateful for the kind support of Dr. Wanyang Sun (Jinan University), Dr. Mingliang Fang (Nanyang Technological University, Singapore), Dr. Dandan Huang (Shanghai Academy of Environmental Sciences, Shanghai, China), and Dr. Chak K. Chan (City University of Hong Kong, Hong Kong, China). The authors also appreciate Hexin Analytical Instrument Co., Ltd., for their generous offer to provide SPIMS 3000 during the measurement campaign. H.H. acknowledges support through the Double-Hundred Talents programme of Shandong Province.

### REFERENCES

- (1) Gligorovski, S.; Abbatt, J. P. D. An Indoor Chemical Cocktail. *Science* **2018**, *359* (6376), 632–633.
- (2) Gligorovski, S.; Li, X.; Herrmann, H. Indoor (Photo)Chemistry in China and Resulting Health Effects. *Environ. Sci. Technol.* **2018**, *52* (19), 10909–10910.
- (3) Wang, L.; Xiang, Z.; Stevanovic, S.; Ristovski, Z.; Salimi, F.; Gao, J.; Wang, H.; Li, L. Role of Chinese Cooking Emissions on Ambient Air Quality and Human Health. *Sci. Total Environ.* **2017**, *589*, 173–181.
- (4) Huang, Y.; Ho, S. S. H.; Ho, K. F.; Lee, S. C.; Yu, J. Z.; Louie, P. K. Characteristics and Health Impacts of VOCs and Carbonyls Associated with Residential Cooking Activities in Hong Kong. *J. Hazard. Mater.* **2011**, *186* (1), 344–351.
- (5) Kim, C.; Gao, Y. T.; Xiang, Y. B.; Barone-Adesi, F.; Zhang, Y.; Hosgood, H. D.; Ma, S.; Shu, X. O.; Ji, B. T.; Chow, W. H.; et al. Home Kitchen Ventilation, Cooking Fuels, and Lung Cancer Risk in a Prospective Cohort of Never Smoking Women in Shanghai, China. *Int. J. Cancer* **2014**, *136* (3), 632–638.
- (6) Schauer, J. J.; Kleeman, M. J.; Cass, G. R.; Simoneit, B. R. T. Measurement of Emissions from Air Pollution Sources. 4. C1-C27 Organic Compounds from Cooking with Seed Oils. *Environ. Sci. Technol.* **2002**, *36*, 567–575.

- (7) Klein, F.; Platt, S. M.; Farren, N. J.; Detournay, A.; Bruns, E. A.; Bozzetti, C.; Daellenbach, K. R.; Kilic, D.; Kumar, N. K.; Pieber, S. M.; et al. Characterization of Gas-Phase Organics Using Proton Transfer Reaction Time-of-Flight Mass Spectrometry: Cooking Emissions. *Environ. Sci. Technol.* **2016**, *50*, 1243–1250.

- (8) Cheng, S.; Wang, G.; Lang, J.; Wen, W.; Wang, X.; Yao, S. Characterization of Volatile Organic Compounds from Different Cooking Emissions. *Atmos. Environ.* **2016**, *145*, 299–307.

- (9) Liu, T.; Liu, Q.; Li, Z.; Huo, L.; Chan, M. N.; Li, X.; Zhou, Z.; Chan, C. K. Emission of Volatile Organic Compounds and Production of Secondary Organic Aerosol from Stir-Frying Spices. *Sci. Total Environ.* **2017**, *599–600*, 1614–1621.

- (10) Zhang, D. C.; Liu, J. J.; Jia, L. Z.; Wang, P.; Han, X. Speciation of VOCs in the Cooking Fumes from Five Edible Oils and Their Corresponding Health Risk Assessments. *Atmos. Environ.* **2019**, *211*, 6–17.

- (11) Bartolomei, V.; Gomez Alvarez, E.; Wittmer, J.; Tlili, S.; Strekowski, R.; Temime-Roussel, B.; Quivet, E.; Wortham, H.; Zetzsch, C.; Kleffmann, J.; et al. Combustion Processes as a Source of High Levels of Indoor Hydroxyl Radicals through the Photolysis of Nitrous Acid. *Environ. Sci. Technol.* **2015**, *49* (11), 6599–6607.

- (12) Zhou, S.; Young, C. J.; Vandenboer, T. C.; Kowal, S. F.; Kahan, T. F. Time-Resolved Measurements of Nitric Oxide, Nitrogen Dioxide, and Nitrous Acid in an Occupied New York Home. *Environ. Sci. Technol.* **2018**, *52* (15), 8355–8364.

- (13) Collins, D. B.; Hems, R. F.; Zhou, S.; Wang, C.; Grignon, E.; Alavy, M.; Siegel, J. A.; Abbatt, J. P. D. Evidence for Gas-Surface Equilibrium Control of Indoor Nitrous Acid. *Environ. Sci. Technol.* **2018**, *52* (21), 12419–12427.

- (14) Liu, J.; Li, S.; Zeng, J.; Mekic, M.; Yu, Z.; Zhou, W.; Loisel, G.; Gandolfo, A.; Song, W.; Wang, X.; et al. Assessing Indoor Gas Phase Oxidation Capacity through Real-Time Measurements of HONO and NO<sub>x</sub> in Guangzhou, China. *Environ. Sci. Process. Impacts* **2019**, *21*, 1393–1402.

- (15) Gandolfo, A.; Gligorovski, V.; Bartolomei, V.; Tlili, S.; Gómez Alvarez, E.; Wortham, H.; Kleffmann, J.; Gligorovski, S. Spectrally Resolved Actinic Flux and Photolysis Frequencies of Key Species within an Indoor Environment. *Build. Environ.* **2016**, *109*, 50–57.

- (16) Kowal, S. F.; Allen, S. R.; Kahan, T. F. Wavelength-Resolved Photon Fluxes of Indoor Light Sources: Implications for HO<sub>x</sub> Production. *Environ. Sci. Technol.* **2017**, *51* (18), 10423–10430.

- (17) Gomez Alvarez, E.; Amedro, D.; Afif, C.; Gligorovski, S.; Schoemaeker, C.; Fittschen, C.; Doussin, J. F.; Wortham, H. Unexpectedly High Indoor Hydroxyl Radical Concentrations Associated with Nitrous Acid. *Proc. Natl. Acad. Sci. U. S. A.* **2013**, *110* (33), 13294–13299.

- (18) Emmerson, K. M.; Carslaw, N.; Pilling, M. J. Urban Atmospheric Chemistry during the PUMA Campaign 2: Radical Budgets for OH, HO<sub>2</sub> and RO<sub>2</sub>. *J. Atmos. Chem.* **2005**, *52* (2), 165–183.

- (19) Ren, X.; Brune, W. H.; Mao, J.; Mitchell, M. J.; Leshner, R. L.; Simpas, J. B.; Metcalf, A. R.; Schwab, J. J.; Cai, C.; Li, Y.; et al. Behavior of OH and HO<sub>2</sub> in the Winter Atmosphere in New York City. *Atmos. Environ.* **2006**, *40* (Suppl. 2), 252–263.

- (20) Elshorbany, Y. F.; Kleffmann, J.; Kurtenbach, R.; Lissi, E.; Rubio, M.; Villena, G.; Gramsch, E.; Rickard, A. R.; Pilling, M. J.; Wiesen, P. Seasonal Dependence of the Oxidation Capacity of the City of Santiago de Chile. *Atmos. Environ.* **2010**, *44* (40), 5383–5394.

- (21) Berndt, T.; Richters, S.; Jokinen, T.; Hyttinen, N.; Kurtén, T.; Otkjær, R. V.; Kjaergaard, H. G.; Stratmann, F.; Herrmann, H.; Sipilä, M.; et al. Hydroxyl Radical-Induced Formation of Highly Oxidized Organic Compounds. *Nat. Commun.* **2016**, *7*, 13677.

- (22) Gligorovski, S.; Weschler, C. J. The Oxidative Capacity of Indoor Atmospheres. *Environ. Sci. Technol.* **2013**, *47* (24), 13905–13906.

- (23) Farmer, D. K.; Vance, M. E.; Abbatt, J. P. D.; Abeleira, A.; Alves, M. R.; Arata, C.; Boedicker, E.; Bourne, S.; Cardoso-Saldaña, F.; Corsi, R.; et al. Overview of HOMEChem: House Observations of

Microbial and Environmental Chemistry. *Environ. Sci. Process. Impacts* **2019**, *21* (8), 1280–1300.

(24) Liu, T.; Wang, Z.; Huang, D. D.; Wang, X.; Chan, C. K. Significant Production of Secondary Organic Aerosol from Emissions of Heated Cooking Oils. *Environ. Sci. Technol. Lett.* **2018**, *5*, 32–37.

(25) Lu, F.; Shen, B.; Yuan, P.; Li, S.; Sun, Y.; Mei, X. The Emission of PM<sub>2.5</sub> in Respiratory Zone from Chinese Family Cooking and Its Health Effect. *Sci. Total Environ.* **2019**, *654*, 671–677.

(26) Tejero Rioseras, A.; Garcia Gomez, D.; Ebert, B. E.; Blank, L. M.; Ibáñez, A. J.; Sinues, P. M. L. Comprehensive Real-Time Analysis of the Yeast Volatilome. *Sci. Rep.* **2017**, *7* (1), 1–9.

(27) Singh, K. D.; Tancev, G.; Decrue, F.; Usemann, J.; Appenzeller, R.; Barreiro, P.; Jaumà, G.; Macia Santiago, M.; Vidal de Miguel, G.; Frey, U.; et al. Standardization Procedures for Real-Time Breath Analysis by Secondary Electrospray Ionization High-Resolution Mass Spectrometry. *Anal. Bioanal. Chem.* **2019**, *411* (19), 4883–4898.

(28) Gaugg, M. T.; Gomez, D. G.; Barrios-Collado, C.; Vidal-de-Miguel, G.; Kohler, M.; Zenobi, R.; Martínez-Lozano Sinues, P. Expanding Metabolite Coverage of Real-Time Breath Analysis by Coupling a Universal Secondary Electrospray Ionization Source and High Resolution Mass Spectrometry — a Pilot Study on Tobacco Smokers. *J. Breath Res.* **2016**, *10* (1), 016010.

(29) Elshorbany, Y. F.; Kurtenbach, R.; Wiesen, P.; Lissi, E.; Rubio, M.; Villena, G.; Gramsch, E.; Rickard, A. R.; Pilling, M. J.; Kleffmann, J. Oxidation Capacity of the City Air of Santiago, Chile. *Atmos. Chem. Phys.* **2009**, *9* (6), 2257–2273.

(30) Li, X.; Huang, D. D.; Du, R.; Zhang, Z. J.; Chan, C. K.; Huang, Z. X.; Zhou, Z. Real-Time Breath Analysis by Using Secondary Nano-electrospray Ionization Coupled to High Resolution Mass Spectrometry. *J. Visualized Exp.* **2018**, *2018* (133), 1–6.

(31) Wolf, J. C.; Schaer, M.; Siegenthaler, P.; Zenobi, R. Direct Quantification of Chemical Warfare Agents and Related Compounds at Low Ppt Levels: Comparing Active Capillary Dielectric Barrier Discharge Plasma Ionization and Secondary Electrospray Ionization Mass Spectrometry. *Anal. Chem.* **2015**, *87* (1), 723–729.

(32) Hughey, C. A.; Hendrickson, C. L.; Rodgers, R. P.; Marshall, A. G.; Qian, K. Kendrick Mass Defect Spectrum: A Compact Visual Analysis for Ultrahigh-Resolution Broadband Mass Spectra. *Anal. Chem.* **2001**, *73* (19), 4676–4681.

(33) Kourtchev, I.; O'Connor, I. P. O.; Giorio, C.; Fuller, S. J.; Kristensen, K.; Maenhaut, W.; Wenger, J. C.; Sodeau, J. R.; Glasius, M.; Kalberer, M. Effects of Anthropogenic Emissions on the Molecular Composition of Urban Organic Aerosols: An Ultrahigh Resolution Mass Spectrometry Study. *Atmos. Environ.* **2014**, *89*, 525–532.

(34) Liu, X. J.; Jin, Q. Z.; Liu, Y. F.; Huang, J. H.; Wang, X. G.; Mao, W. Y.; Wang, S. S. Changes in Volatile Compounds of Peanut Oil during the Roasting Process for Production of Aromatic Roasted Peanut Oil. *J. Food Sci.* **2011**, *76* (3), C404–C412.

(35) Hu, W.; Zhang, L.; Li, P.; Wang, X.; Zhang, Q.; Xu, B.; Sun, X.; Ma, F.; Ding, X. Characterization of Volatile Components in Four Vegetable Oils by Headspace Two-Dimensional Comprehensive Chromatography Time-of-Flight Mass Spectrometry. *Talanta* **2014**, *129*, 629–635.

(36) Gardner, H. W. Oxygen Radical Chemistry of Polyunsaturated Fatty Acids. *Free Radical Biol. Med.* **1989**, *7* (1), 65–86.

(37) Choe, E.; Min, D. B. Comprehensive Reviews in Food Science and Food Safety Mechanisms and Factors for Edible Oil Oxidation. *Compr. Rev. Food Sci. Food Saf.* **2006**, *5*, 169–186.

(38) Wang, C. K.; Chang, L. W.; Chang, H.; Yang, C. H.; Tsai, M. H.; Tsai, H. T.; Lin, P. Pulmonary Changes Induced by Trans, Trans-2,4-Decadienal, a Component of Cooking Oil Fumes. *Eur. Respir. J.* **2010**, *35* (3), 667–675.

(39) Young, S. C.; Chang, L. W.; Lee, H. L.; Tsai, L. H.; Liu, Y. C.; Lin, P. DNA Damage Induced by Trans, Trans-2,4-Decadienal (Tt-DDE), a Component of Cooking Oil Fume, in Human Bronchial Epithelial Cells. *Environ. Mol. Mutagen.* **2010**, *51*, 315–321.

(40) Mu, L.; Liu, L.; Niu, R.; Zhao, B.; Shi, J.; Li, Y.; Swanson, M.; Scheider, W.; Su, J.; Chang, S. C.; et al. Indoor Air Pollution and Risk

of Lung Cancer among Chinese Female Non-Smokers. *Cancer Causes Control* **2013**, *24* (3), 439–450.

(41) Vranová, J.; Ciesarová, Z. Furan in Food — a Review. *Czech J. Food Sci.* **2009**, *27* (1), 1–10.

(42) Rogge, W. F.; Hildemann, L. M.; Mazurek, M. A.; Cass, G. R.; Simoneit, B. R. T. Sources of Fine Organic Aerosol. 1. Charbroilers and Meat Cooking Operations. *Environ. Sci. Technol.* **1991**, *25* (6), 1112–1125.

(43) Atkinson, R.; Arey, J. Atmospheric Degradation of Volatile Organic Compounds. *Chem. Rev.* **2003**, *103* (12), 4605–4638.

(44) Ho, K. F.; Lee, S. C.; Ho, S. S. H.; Kawamura, K.; Tachibana, E.; Cheng, Y.; Zhu, T. Dicarboxylic Acids, Ketocarboxylic Acids,  $\alpha$ -Dicarbonyls, Fatty Acids, and Benzoic Acid in Urban Aerosols Collected during the 2006 Campaign of Air Quality Research in Beijing (CAREBeijing - 2006). *J. Geophys. Res.* **2010**, *115*, D19312.

(45) Ahn, J. H.; Szulejko, J. E.; Kim, K. H.; Kim, Y. H.; Kim, B. W. Odor and VOC Emissions from Pan Frying of Mackerel at Three Stages: Raw, Well-Done, and Charred. *Int. J. Environ. Res. Public Health* **2014**, *11* (11), 11753–11771.

(46) Murphy, S. M.; Sorooshian, A.; Kroll, J. H.; Ng, N. L.; Chhabra, P.; Tong, C.; Surratt, J. D.; Knipping, E.; Flagan, R. C.; Seinfeld, J. H. Secondary Aerosol Formation from Atmospheric Reactions of Aliphatic Amines. *Atmos. Chem. Phys.* **2007**, *7*, 2313–2337.

(47) Silva, P. J.; Erupe, M. E.; Price, D.; Elias, J.; Malloy, Q. G. J.; Li, Q.; Warren, B.; Cocker, D. R. Trimethylamine as Precursor to Secondary Organic Aerosol Formation via Nitrate Radical Reaction in the Atmosphere. *Environ. Sci. Technol.* **2008**, *42* (13), 4689–4696.

(48) Tang, X.; Price, D.; Praske, E.; Lee, S. A.; Shattuck, M. A.; Purvis-Roberts, K.; Silva, P. J.; Asa-Awuku, A.; Cocker, D. R. NO<sub>3</sub> Radical, OH Radical and O<sub>3</sub>-Initiated Secondary Aerosol Formation from Aliphatic Amines. *Atmos. Environ.* **2013**, *72* (3), 105–112.

(49) Zhang, X.; Barraza, K. M.; Upton, K. T.; Beauchamp, J. L. Time Resolved Study of Hydroxyl Radical Oxidation of Oleic Acid at the Air-Water Interface. *Chem. Phys. Lett.* **2017**, *683*, 76–82.

(50) Nah, T.; Kessler, S. H.; Daumit, K. E.; Kroll, J. H.; Leone, S. R.; Wilson, K. R. OH-Initiated Oxidation of Sub-Micron Unsaturated Fatty Acid Particles. *Phys. Chem. Chem. Phys.* **2013**, *15*, 18649–18663.

(51) He, X.; Leng, C.; Pang, S.; Zhang, Y. Kinetics Study of Heterogeneous Reactions of Ozone with Unsaturated Fatty Acid Single Droplets Using Micro-FTIR Spectroscopy. *RSC Adv.* **2017**, *7* (6), 3204–3213.

(52) Hoffmann, T.; Bandur, R.; Hoffmann, S.; Warscheid, B. On-Line Characterization of Gaseous and Particulate Organic Analytes Using Atmospheric Pressure Chemical Ionization Mass Spectrometry. *Acta, Part B* **2002**, *57*, 1635–1647.

(53) Zahardis, J.; Petrucci, G. A. The Oleic Acid-Ozone Heterogeneous Reaction System: Products, Kinetics, Secondary Chemistry, and Atmospheric Implications of a Model System - A Review. *Atmos. Chem. Phys.* **2007**, *7* (5), 1237–1274.

(54) Kawamura, K.; Seméré, R.; Imai, Y.; Fujii, Y.; Hayashi, M. Water Soluble Dicarboxylic Acids and Related Compounds in Antarctic Aerosols. *J. Geophys. Res. Atmos.* **1996**, *101* (13), 18721–18728.

(55) Kawamura, K.; Kasukabe, H.; Barrie, L. A. Source and Reaction Pathways of Dicarboxylic Acids, Ketoacids and Dicarbonyls in Arctic Aerosols: One Year of Observations. *Atmos. Environ.* **1996**, *30* (10–11), 1709–1722.

(56) Won, Y.; Waring, M. S.; Rim, D. Understanding the Spatial Heterogeneity of Indoor OH and HO<sub>2</sub> Due to Photolysis of HONO Using Computational Fluid Dynamics (CFD) Simulation. *Environ. Sci. Technol.* **2019**, *53*, 14470.